Soft Matter

PAPER

Effect of confinement on electric field induced orientation of a nematic liquid crystal†

Cite this: *Soft Matter*, 2014, **10**, 2110

Shinya Nakano,[a] Masashi Mizukami[a] and Kazue Kurihara*[ab]

We report the effect of confinement on the electric field induced orientation of a nematic liquid crystal, 4-cyano-4′-hexylbiphenyl (6CB), between mica surfaces. The resonance shear measurement was employed for monitoring changes in the viscosity of 6CB at various surface separation distances (D) with and without an applied electric field. The viscosity depended on the surface separations, and the behaviour for $D <$ *ca.* 20 nm was quite different from that at $D >$ *ca.* 20 nm. For $D >$ *ca.* 20 nm, the viscosity values obtained in the presence of the electric field (ac 1 kHz, 1.87 kV mm^{-1}, homeotropic orientation) were *ca.* 2 times higher than the values obtained without the electric field (0 kV mm^{-1}, planar orientation) due to the difference in the molecular orientation, and were nearly constant. At $D <$ *ca.* 20 nm, the viscosity of 6CB both with and without the electric field sharply increased and they merged into an identical value at $D = 12.5 \pm 1.3$ nm (D_c), then exhibited a plateau up to $D = 6$ nm. With the decreasing distance below 6 nm, the viscosity of confined 6CB both with and without the electric field further increased up to more than 100 N s m^{-1} at the hard wall thickness of $D =$ *ca.* 4.0 nm. These results indicated that 6CB molecules both with and without the electric field had the same orientation at $D < D_c$. The most likely orientation of 6CB was parallel to the surfaces because 6CB was originally in a planar orientation on the mica surface. These results demonstrated for the first time that the effect of confinement exceeded the electric field, thus 6CB molecules could not change their orientation under the electric field at the surface separation below D_c.

Received 29th October 2013
Accepted 3rd January 2014

DOI: 10.1039/c3sm52744a

www.rsc.org/softmatter

1. Introduction

Liquids confined in molecular-scale spaces, such as a narrow gap between two solid surfaces and spaces in nanoporous materials, show markedly different properties from the bulk state due to the spatial limitation and the interactions between liquid molecules and solid surfaces.[1–6] Thus, understanding the behaviour of confined liquids is of increasing importance for both fundamental sciences and potential applications such as in nano-imprinting and nano-chemical devices. Surface force measurement employing the surface force apparatus (SFA) and SFA-based shear measurements have been regarded as useful tools for studying confined liquids.[5–14] Because the SFA can continuously control the surface separation distance (D) from submicron down to a molecular-scale, characterization of the properties of confined liquids is possible with varying D. We have developed the resonance shear measurement (RSM) based on the SFA (Fig. 1) and applied it for evaluating the viscosity and lubricity of confined liquids.[6,11–14] This method utilises the resonance curve of the mechanical top surface unit which sensitively changes depending on the properties of confined liquids, thus it has advantages such as high sensitivity and stability. Liquid crystals (LCs) have been studied in confined spaces,[6–11] because their anisotropic nature in the liquid state and useful applications in displays and other devices[15,16] are attractive from both the basic and applied scientific points of view. Typical behavior of other confined liquids, the oscillation force[7,8] and the increase in viscosity under confinement[6] have also been reported for LCs.

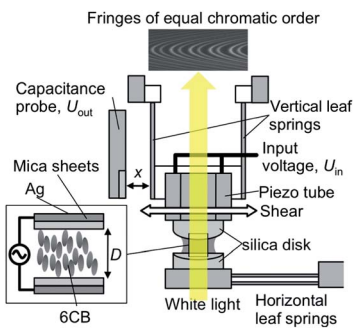

Fig. 1 Schematic illustration of the resonance shear measurement system.

[a]*Institute of Multidisciplinary Research for Advanced Materials, Tohoku University, JST-CREST, Katahira 2-1-1, Aoba-ku, Sendai 980-8577, Japan. E-mail: kurihara@tagen.tohoku.ac.jp*

[b]*WPI-Advanced Institute for Materials Research (AIMR), Tohoku University, Katahira 2-1-1, Aoba-ku, Sendai 980-8577, Japan*

† Electronic supplementary information (ESI) available. See DOI: 10.1039/c3sm52744a

In typical LC devices, the orientation of surface-aligned LC molecules (*e.g.*, planar orientation) can be changed (*e.g.*, to homeotropic orientation) by applying an electric field. The confinement of LCs in several micrometer thick cells is known to suppress the director fluctuation and to increase the order parameter. They are interpreted as the existence of the boundary layer induced by the surface anchoring and/or the existence of the large correlation length of LCs comparable to the cell thickness.[17,18] Therefore, it should be interesting to determine the orientational behaviour of LCs confined in a nanometer gap between two solid surfaces under the effect of an applied electric field. Study of the spatial confinement and the electric field effects on LCs in nanometer-scale spaces should help for further understanding the confinement effect. However, to the best of our knowledge, there have been no such studies.

In this study, we performed RSM to investigate the confined LCs between the mica surfaces under an electric field. We used 4-cyano-4′-hexylbiphenyl (6CB) as the LC sample and mica as the substrate because 6CB has a planar orientation on a clean mica surface[8] and can be oriented along the direction of an applied electric field (homeotropic orientation) due to its positive dielectric anisotropy ($\Delta\varepsilon = \varepsilon_{\parallel} - \varepsilon_{\perp} = 16.7 - 6.9 = 9.8$).[19] When the confinement effect became significant, we found that 6CB between the mica surfaces did not align along the applied electric field. To the best of our knowledge, this is the first report of the influence of confinement on the electric field induced orientation of a nematic LC.

2. Experimental

2.1 Liquid crystal

6CB (4-cyano-4′-hexyl-biphenyl) from Merck was used as received. 6CB is in a crystalline phase below 14.5 °C, a nematic phase at 14.5–29.4 °C, and an isotropic phase above 29.4 °C.

2.2 Polarizing optical microscopy observation of a liquid crystal cell

The orientational behavior of 6CB between the mica surfaces under an applied electric field was initially examined by observing a homemade LC cell, which consisted of two back-silvered mica sheets and had a cell thickness of 12 μm, using a polarizing optical microscope (Olympus, BXP) with crossed polarisers. The crystallographic axes of the two mica sheets were aligned parallel to each other and a polariser was set parallel to one of the crystallographic axes of the mica sheets. A dc or ac voltage was applied between the silver layers on the backside of the mica sheets. All the measurements were carried out at room temperature.

2.3 Resonance shear measurement (RSM)

RSM was performed in a manner similar to that previously described.[6,11–14] Fig. 1 shows a schematic illustration of the RSM system. The upper surface was hung by a pair of leaf springs and laterally moved by a four-sectored piezo tube, which was driven by applying sinusoidal voltages (amplitude $U_{in} = \pm 1$ V, frequency f typically within the range of 10–100 Hz) to the two opposite electrodes using the DAQ (data acquisition) board from National Instruments. The deflection of the leaf spring was detected using a capacitance probe (Japan ADE, MicroSense 3401HR) as its output voltage (U_{out}, sensitivity: 2.518 μm V^{-1}). The amplitude ratio U_{out}/U_{in} *vs.* ω ($= 2\pi f$) was plotted as the resonance curve, in which the U_{out}/U_{in} at the resonance peak and its frequency ω_{res} reflected the sample properties, such as viscosity and friction. The lower surface was supported by double cantilever springs. The backside of the mica sheets (3.2–4.9 μm thickness in this study) used as substrates was coated by vacuum deposited silver layers of 50 nm in thickness to produce interference fringes, and then glued onto cylindrical quartz discs (a radius of curvature (R) = 20 mm) using epoxy resin (Shell, Epikote 1004). The surface separation distance between mica surfaces (D) was determined using the fringes of equal chromatic order (FECO) with a resolution of 0.1 nm.[20] The silver layers on the backside of mica sheets were also used as electrodes for applying the electric field to the 6CB. Wires were carefully connected to the silver layers on the backside of the mica sheets, which were glued onto cylindrical silica disks, using conductive epoxy resin (ITW Chemtronics, CW2400). The electric field was applied using a function generator (Wavetek, 10 MHz DDS Function Generator Model 29) through an amplifier (Echo Electronics, ENP-2001A). A droplet of 6CB (about 10 μL) was injected between the upper and lower mica surfaces.

In order to quantitatively discuss the viscosity of confined 6CB, the resonance curves (U_{out}/U_{in} *vs.* ω) were fitted by the derived equation based on a physical model following a previously reported procedure.[13] Fig. 2 illustrates the physical model employed. In this model, b_1 and b_3 are the damping parameters of the upper and lower units, k_1 and k_3 are the spring constants of the upper and lower units, and b_2 and k_2 are the viscous damping and elastic parameters of the confined sample, respectively. The parameters m_1 and m_2 correspond to the mass of the upper and lower units, respectively. We first determined the apparatus parameters of the upper and lower units by fitting the reference resonance curves (AS and MC curves). For the analysis of the resonance curve of AS, the parameters of the sample b_2 and k_2 and the lower unit b_3, k_3, and m_2 are zero. Under these conditions, the theoretical resonance curve of the AS peak derived from the corresponding equation of motion is written as

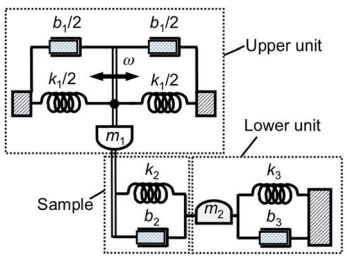

Fig. 2 A physical model of the resonance shear apparatus for analysing resonance curves to obtain the damping parameter of 6CB.

$$\frac{U_{out}}{U_{in}} = \frac{C}{m_1}\left[\left(\frac{1}{\alpha}\frac{k_1}{m_1} - \omega^2\right) + \left(\frac{b_1}{m_1}\right)^2\omega^2\right]^{-1/2} \quad (1)$$

where C is an apparatus constant and α is a parameter related to the lateral movement of the upper surface (x_1) with respect to the movement of the end of the vertical leaf spring ($x_{measured}$) ($x_1 = \alpha x_{measured}$). The equation of the resonance curves for the MC and those in the presence of 6CB can be written as

$$\frac{U_{out}}{U_{in}} = \frac{C}{\alpha}\sqrt{\frac{(K_2 - m_2\omega^2)^2 + \omega^2 B_2{}^2}{\left[(K_1 - m_1\omega^2)(K_2 - m_2\omega^2) - \omega^2 B_1 B_2 - k_2{}^2 + b_2{}^2\omega^2\right]^2 + \omega^2[(K_1 - m_1\omega^2)B_2 + (K_2 - m_2\omega^2)B_1 - 2k_2 b_2]^2}} \quad (2)$$

where $B_1 = b_1 + b_2$, $B_2 = b_2 + b_3$, $K_1 = k_1/\alpha + k_2$, and $K_2 = k_2 + k_3$. To determine the parameters of the lower unit, the resonance curve for MC was fitted using eqn (2) in which the parameters for a sample (b_2 and k_2) were deleted to adjust the equation to the no slip condition ($x_1 = x_2$) and the fixed upper unit parameters (b_1 and m_1) obtained from the AS curve were used. Finally, the parameters of the 6CB samples (b_2 and k_2) were determined by fitting the resonance curves in the presence of 6CB at various surface separations using eqn (2) and the fixed apparatus parameters.

3. Results and discussion

3.1 Polarizing optical microscopy observation of the liquid crystal under an electric field

In order to investigate the orientational behaviour of 6CB between the mica surfaces by applying an electric field across a mica substrate, polarizing optical microscopy observations of the LC in a homemade cell were initially performed. The orientation of 6CB was monitored by observing orthoscopic and conoscopic images. Before applying the voltage (planar orientation), a bright image without texture was observed (see ESI, Fig. S1(a) and (b)†). At the beginning of our study, we used the dc voltage to orient 6CB molecules, and by increasing a dc voltage up to 80 V, the orthoscopic image became dark and the conoscopic image gradually showed the typical interference pattern which indicated the homeotropic orientation of the nematic LC. However, when the dc voltage was kept constant, the dark image returned back to a bright image in seconds. This indicated that a voltage drop occurred and the orientation returned back to planar again. When ac voltages of 14 and 28 V (sinusoidal wave, 1 kHz) were applied, the dark image and the conoscopic interference pattern were maintained (Fig. S1(c)–(f)†). Therefore, to avoid the voltage drop with time, we used an ac voltage for the RSM.

3.2 RSM determination of ac voltage to induce the homeotropic orientation of 6CB

RSM was performed at the fixed surface separation of 322 ± 5 nm under various applied voltages to determine the amplitude of the applied ac voltage to induce the homeotropic orientation of 6CB. Nematic LCs consisting of rod-like molecules are known to exhibit higher viscosity in the homeotropic orientation than in the planar orientation against shear flow.[21] Thus, the orientational change in the nematic LCs can be detected by monitoring the viscosity of 6CB.[13] The decrease in the resonance amplitude corresponds to the increase in the viscosity of liquids between solid surfaces. Fig. 3 shows the resonance curves for 6CB between the mica surfaces measured at various ac voltages. The inset of Fig. 3 shows the voltage dependence of the resonance amplitude at the resonance peak (ω = 206 rad s^{-1}). As the applied ac voltage increased, the resonance amplitude gradually decreased from the value at 7 V and became almost constant at *ca.* 28 V. The decrease in the resonance amplitude with the increasing applied voltage indicated that the orientation of 6CB changed from planar at 0 V to homeotropic at 28 V because the viscosity of 6CB in the homeotropic alignment is known to be larger than that of the planar orientation.[21] The orientational change from planar to homeotropic was continuous and was not like Freederick's transition. It was difficult to estimate the actual electric field strength within the 6CB film because the surfaces had a crossed cylinder geometry. By assuming a plate electrode geometry and the capacitors in series (mica–6CB–mica),[22] the electric field (E) strength needed to induce the homeotropic orientation in 6CB between the mica surfaces was estimated to be 1.87 kV mm^{-1} using the following equation.

$$E = \frac{\varepsilon_{mica} V}{2\varepsilon_{6CB} t_{mica} + \varepsilon_{mica} D} \quad (3)$$

For this calculation, the surface separation distance D = 322 nm, the mica thickness t_{mica} = 3.1 μm, the dielectric constant of mica ε_{mica} = 7.0,[23] and the dielectric constant of 6CB, ε_{6CB} = ($\varepsilon_{||}$ = 16.7)[19] were used. In the following measurement, the applied voltage was adjusted in order to apply the electric field strength of 1.87 kV mm^{-1} on 6CB based on the mica thickness.

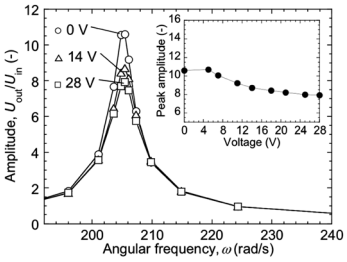

Fig. 3 Resonance curves of 6CB confined between mica surfaces at various amplitudes of ac voltage, 0 V (circles), 14 V (triangles), and 28 V (squares). The inset shows the voltage dependence of the resonance amplitude at the peak (ω = 206 rad s^{-1}). The mica thickness used in this measurement was 3.1 μm, and the surface separation was fixed at 322 ± 5 nm.

3.3 RSM for 6CB at various distances under an applied electric field

The effect of confinement on the electric field induced orientation of 6CB was investigated by performing the RSM as a function of the surface separation without and with the presence of an electric field. Fig. 4(a) shows the typical resonance curves obtained for 6CB without the electric field. Two reference states, the curve for the separation in air (AS) and that for the mica–mica contact (MC) in air, are also plotted for convenience. For the AS curve, the peak frequency, ω_{AS}, was characterized by the mass and the spring constant of the upper surface unit. On the other hand, for the MC curve, the upper and the lower surface moved together in a strong adhesion contact. Thus, the resonance frequency of the MC curve, ω_{MC}, shifted to a higher frequency determined due to the contribution of the mass and spring constant of lower surface units. At $D = 369$ nm after the injection of 6CB, the resonance peak was observed at an angular frequency of 206 rad s^{-1}, the same frequency as that of the AS peak whilst the intensity of U_{out}/U_{in} was 12.9, *ca.* 39% of the AS peak intensity. The decrease in the peak intensity compared to the AS peak was due to the bulk viscosity of 6CB in a planar orientation. When the surfaces approached, the peak intensity gradually decreased, and a significant decrease in the peak intensity started at $D < 17.2$ nm. At $D = 12.8$ nm, a broad peak emerged and then the peak position started to shift toward a high angular frequency. At surface separations shorter than 7.4 nm, the resonance peak appeared in a high angular frequency region, indicating transmission of the shear force to the lower surface due to the further increase in the viscosity of confined 6CB. The peak intensity gradually increased upon decreasing the surface separation. At $D = 4.1$ nm (the smallest surface separation we could reach in this study), the peak intensity U_{out}/U_{in} increased to 10.8 which was *ca.* 61% of the MC peak, and no further increase in the peak intensity was observed by further increasing the normal load. These changes in the resonance curve indicated that the viscosity of 6CB confined between mica surfaces sharply increased at $D = 17.2$–4.1 nm.[24] As described in the Introduction, the increase in the viscosity of a liquid crystal confined in a micrometer thick cell is related to the existence of the boundary layer induced by the surface anchoring, suppression of the director fluctuation and/or the existence of the correlation length comparable to the surface separation.[17,18] The viscosity increase of 6CB observed in this study occurred at $D = 17.2$–4.1 nm, which was much narrower by more than three orders of magnitude than a micrometer thick gap (see Fig. 5), which cannot be explained by the inherent properties of large correlation length in bulk 6CB. Therefore, the viscosity increase in this case should be related to the increase in the order parameter and suppression of director fluctuation due to the nano-confinement. Contribution of the boundary layer induced by the surface anchoring could not be excluded within our experiment.

Fig. 4(b) shows the typical resonance curves obtained for 6CB under the ac voltage (frequency 1 kHz, amplitude 28 V) at various surface separations. The electric field strength E within 6CB was regarded to be almost constant on approaching surfaces because the thickness of the intervening mica sheets (3.1 μm) was much greater than the thickness change in a 6CB thin film. For example, the electric field strength was calculated to be $E = 1.87$ kV mm^{-1} at $D = 357$ nm and $E = 1.91$ kV mm^{-1} at $D = 20.2$ nm. At $D = 357$ nm, the resonance peak was observed at a frequency of 206 rad s^{-1}, the same frequency as that of the AS peak, and the intensity of U_{out}/U_{in} was 10.0 (*ca.* 30% of the AS peak intensity). As shown in Fig. 3, the smaller peak intensity

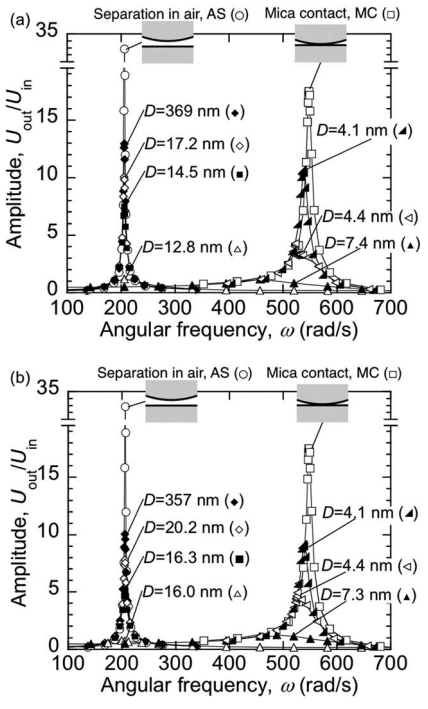

Fig. 4 Resonance curves of 6CB confined between mica surfaces at various surface separations (a) without the electric field (0 kV mm^{-1}) and (b) with the electric field (1.87–1.91 kV mm^{-1}, 1 kHz). The resonance curves for the surfaces separated in air and for the mica–mica surface contact in air are also shown.

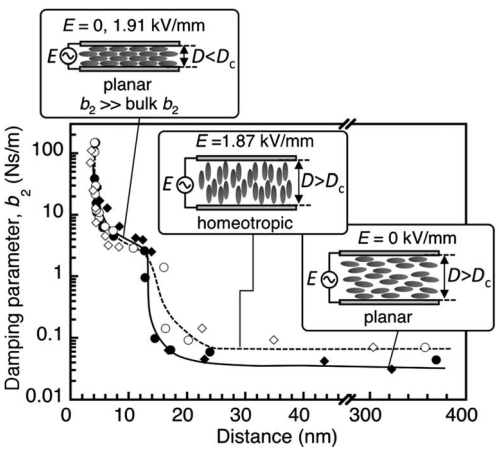

Fig. 5 Surface separation dependence of the damping parameter b_2 of 6CB with the electric field (open symbols) and without the electric field (filled symbols). Solid and dashed lines are drawn as a guide to the eye.

under the electric field indicated that 6CB was in the homeotropic orientation. On the approaching surfaces down to D = 20.2 nm, the peak intensity gradually decreased, then significantly decreased at D < 20.2 nm, and at D = 16.0 nm, the peak became weak (U_{out}/U_{in} < 1) and broad. Similar to the situation observed without the electric field (Fig. 4(a)), at D < 7.3 nm, the resonance peak shifted to the higher angular frequency region, thus indicating transmission of the shear force to the lower surface due to the further increase in the viscosity of confined 6CB. The peak intensity gradually increased with further decrease in surface separation. The smallest D = 4.1 nm we could reach in this study was the same as that observed without the electric field, and the maximum peak intensity (U_{out}/U_{in}) measured at D = 4.1 nm was 9.1 (*ca.* 52% of the MC peak).

The comparison of the resonance curves obtained with and without the electric field can be summarized as follows: (1) at large D (>*ca.* 20 nm), the viscosity expected from the peak intensity was larger when the electric field was applied, indicating that the homeotropic orientation could be induced by the electric field at Ds down to *ca.* 20 nm and (2) at small D (<*ca.* 7 nm), where the peak shifted to higher frequency, the resonance curves obtained with and without the electric field were similar, indicating that the properties of 6CB were independent of the electric field.[25] These results suggested that the response of 6CB to the electric field was suppressed when they were confined in a small gap between mica surfaces. In order to compare the properties of confined 6CB with and without the electric field at various Ds, the viscous damping parameter of 6CB b_2 was obtained by analysing the resonance curves and plotted against D.

3.4 Confinement effect on the orientation of 6CB under an electric field

The viscous damping parameter b_2 of 6CB confined between mica surfaces was obtained by fitting the resonance curves using eqn (2) derived from the physical model shown in Fig. 2. Fig. 5 shows the damping parameter b_2 of confined 6CB with and without an electric field plotted *versus* the surface separation (D). The results of the different sets of measurements are also plotted to show the reproducibility. At D > *ca.* 20 nm, the viscosity of each case was practically constant independent of the distance, and the damping parameter b_2 of the homeotropic orientation (with the electric field), 0.087 ± 0.023 N s m^{-1}, was about 2 times larger than that of the planar orientation (without the electric field), 0.043 ± 0.009 N s m^{-1}. In general, the viscosity in the homeotropic orientation is about two to four times larger than that in the planar orientation.[21,26,27] The observed b_2 value ratio was similar to the reported ratio. This meant that the orientation of confined 6CB could be changed from planar to homeotropic by applying the electric field at D > *ca.* 20 nm.

On the other hand, at D = 20–13 nm, the viscosity sharply increased with the decreasing distance, and the values with and without the electric field merged into an identical value of 3.1 ± 0.8 N s m^{-1} at D = 12.5 ± 1.3 nm (D_c). At D < D_c, the slope of b_2 *vs.* D became smaller (nearly a plateau). With the decreasing distance below 6 nm, the b_2 values further sharply increased up to more than 100 N s m^{-1} at a hard wall thickness of D = 3.5 ± 0.7 nm with the electric field and D = 4.1 ± 0.1 nm without the electric field, which were identical within the experimental error. The sharp increase in the b_2 values at D < *ca.* 20 nm indicated that the motion of the 6CB molecules became suppressed due to the spatial confinement, which should also suppress the orientational motion of 6CB molecules induced by the electric field. The identical b_2 value obtained with and without the electric field at D < D_c indicated that the confined 6CBs both with and without the electric field had a planar orientation. The orientational energy of 6CB caused by the electric field of 1.91 kV mm^{-1} was estimated to be on the order of 10^{-8} J m^{-2}.[28,29] This value was much smaller than the usual surface anchoring energy of the nematic liquid crystal (~10^{-5} J m^{-2}).[30,31] Therefore, the 6CB molecules confined in the thickness below D_c (12.5 ± 1.3 nm) should be in a planar orientation. This means that at D < D_c, the suppression of motion of 6CBs due to the confinement effect exceeds the electric field effect on the orientation of 6CB. To the best of our knowledge, these results revealed for the first time that the confinement effect exceeds the electric field effect on the orientational motion of liquid crystal molecules between the gap at D < D_c.

4. Conclusion

We performed the resonance shear measurement (RSM) for characterizing the confinement effect on 6CB between the mica surfaces under an applied electric field. We found that the viscosity changes of confined 6CB with and without an electric field at D < *ca.* 20 nm were quite different from those at D > *ca.* 20 nm. For D > *ca.* 20 nm, the damping parameter b_2 values obtained under the electric field (homeotropic orientation) were greater than the values obtained without the electric field (planar orientation) due to the anisotropic viscosity. On the other hand, at D < *ca.* 20 nm, the viscosity sharply increased with the decreasing distance, and the values with and without the electric field merged into an identical value of 3.1 ± 0.8 N s m^{-1} at D = 12.5 ± 1.3 nm (D_c). This indicated that the confined 6CBs had the same orientation, *i.e.*, planar orientation, with and without the electric field due to the suppression of the rotation of 6CB molecules confined in the gap thinner than D_c. To the best of our knowledge, this study revealed for the first time that the orientation of a liquid crystal in a nano-confined space could not be controlled by applying an electric field, and determined the critical surface separation (D_c) where the confinement effect exceeded the electric field effect on the orientation of the liquid crystal. Our results can provide important knowledge for the study of confinement effects on liquids and understanding the effect of the applied electric field in a nanometer-scale space.

Acknowledgements

This research was supported by the Core Research for Evolutional Science and Technology (CREST) program of the Japan Science and Technology Agency (JST) and the "Green Tribology Innovation Network" in the area of Advanced Environmental

Materials of Green Network of Excellence (GRENE) program from the Ministry of Education, Culture, Sports, Science, and Technology of Japan.

References

1 S. Granick, *Science*, 1991, **253**, 1374.
2 H. K. Christenson, *J. Phys.: Condens. Matter*, 2001, **13**, R95.
3 C. Alba-Simionesco, B. Coasne, G. Dosseh, G. Dudziak, K. E. Gubbins, R. Radhakrishnan and M. Sliwinska-Bartkowiak, *J. Phys.: Condens. Matter*, 2006, **18**, R15.
4 R. Busselez, R. Lefort, Q. Ji, F. Affouard and D. Morineau, *Phys. Chem. Chem. Phys.*, 2009, **11**, 11127.
5 S. Perkin, *Phys. Chem. Chem. Phys.*, 2012, **14**, 5052.
6 M. Mizukami, K. Kusakabe and K. Kurihara, *Prog. Colloid Polym. Sci.*, 2004, **128**, 105.
7 R. G. Horn, J. N. Israelachvili and E. Perez, *J. Phys., Lett.*, 1981, **42**, 39.
8 J. Janik, R. Tadmor and J. Klein, *Langmuir*, 1997, **13**, 4466.
9 M. Ruths and S. Granick, *Langmuir*, 2000, **16**, 8368.
10 Y.-K. Cho and S. Granick, *J. Chem. Phys.*, 2003, **119**, 547.
11 C. D. Dushkin and K. Kurihara, *Rev. Sci. Instrum.*, 1998, **69**, 2095.
12 H. Sakuma, K. Otsuki and K. Kurihara, *Phys. Rev. Lett.*, 2006, **96**, 046104.
13 M. Mizukami and K. Kurihara, *Rev. Sci. Instrum.*, 2008, **79**, 113705.
14 K. Ueno, M. Kasuya, M. Watanabe, M. Mizukami and K. Kurihara, *Phys. Chem. Chem. Phys.*, 2010, **12**, 4066.
15 *Handbook of Liquid Crystals, 1*, ed. D. Demus, J. W. Goodby, G. W. Gray, N. Spiess and V. Vill, Wiley-VCH Verlag GmbH, Weinheim, Germany, 1998.
16 S. J. Woltman, G. D. Jay and G. P. Crawford, *Nat. Mater.*, 2007, **6**, 929.
17 P. Sheng, *Phys. Rev. A: At., Mol., Opt. Phys.*, 1982, **26**, 1610.
18 S. Dhara and N. V. Madhusudana, *Eur. Phys. J. E: Soft Matter Biol. Phys.*, 2004, **13**, 401.
19 D. A. Dunmur, M. R. Manterfield, W. H. Miller and J. K. Dunleavy, *Mol. Cryst. Liq. Cryst.*, 1978, **45**, 127.
20 J. N. Israelachvili, *J. Colloid Interface Sci.*, 1973, **44**, 259.
21 M. Miesowicz, *Nature*, 1946, **158**, 27.
22 A. Marino, V. Tkachenko, E. Santamato, N. Bennis, X. Quintana, J. M. Otón and G. Abbate, *J. Appl. Phys.*, 2010, **107**, 073109.
23 J. N. Israelachvili, *Intermolecular and Surface Forces*, Academic, New York, 2nd edn, 1992.
24 The distance range where the viscosity of 6CB increased due to confinement was larger compared with that previously observed (D = 11.7–3.9 nm).[6] This should be related to the smaller input voltage (1 V) to the piezo compared to the value used in the previous one (20 V). When the input voltage becomes smaller, the shear amplitude and shear velocity became smaller, and the shear thinning effect becomes smaller. Thus, the viscosity could start decrease in a larger distance range.
25 At $D < D_c$, we applied a voltage up to the amplitude of 100 V, which corresponded to the electric field of 6.82 kV mm^{-1} across the 6CB layer, the planar–homeotropic transition could not be induced. We avoided applying further high voltage for safety.
26 K. Negita, *J. Chem. Phys.*, 1996, **105**, 7837.
27 J. Janik, J. K. Moscicki, K. Czuprynski and R. Dabrowski, *Phys. Rev. E: Stat. Phys., Plasmas, Fluids, Relat. Interdiscip. Top.*, 1998, **58**, 3251.
28 T. Carlsson and K. Skarp, *Mol. Cryst. Liq. Cryst.*, 1981, **78**, 157.
29 The orientational energy by the electric field was estimated using a equation of $\Gamma = -\frac{\Delta\varepsilon\varepsilon_0}{2}E^2\sin 2\theta$ (J m^{-3}).[28] Here, θ was the angle between the electric field and the director of 6CB. The orientational energy for the unit area (G_{el}) was obtained by multiplying the thickness of the one dimer layer in planar orientation ($G_{el} = \Gamma d$ (J m^{-2}), d = 0.3 nm).
30 L. M. Blinov and V. G. Chigrinov, *Electro-Optic Effects in Liquid Crystal Materials*, Springer, New York, 1994.
31 R. M. S. Ataalla, G. Barbero and L. Komitov, *J. Appl. Phys.*, 2013, **113**, 164501.